Luminosity monitor and low Q^2 tagger for the EIC

Jaroslav Adam

BNL

1st EIC Yellow Report Workshop at Temple University, March 19, 2020

Introduction

- Summary on simulation activities for luminosity monitor and low Q^2 tagger will be given here, with implications to detector requirements
- Technical details are given in backup of this presentation
- Luminosity measurement requires a fast calorimeter (timing resolution much better than bunch spacing) and good energy resolution
- Independent segmentation in vertical and horizontal direction
- Calorimeter for low Q^2 tagger has similar requirements as for luminosity detector
- Needs more precise position resolution - layers of tracking detectors in front of the calorimeter

Concept for luminosity measurement

- Following example of similar detector at ZEUS, HERA
- High luminosity demands two separate methods to count the bremsstrahlung photons:

1. Photon conversion to e^+e^- pairs for precise DIS cross sections
2. Direct, non converted photons for instantaneous collider performance

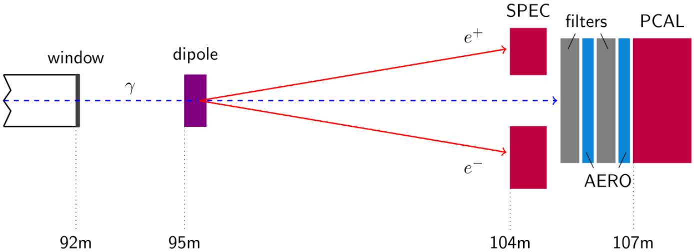

Figure: Layout of ZEUS luminosity detector

- Pairs are detected in spectrometer SPEC, direct photons in photon calorimeter PCAL

Nucl.Instrum.Meth. A744 (2014) 80-90, Nucl.Instrum.Meth. A565 (2006) 572-588

Luminosity monitor and low Q^2 tagger in the IR layout

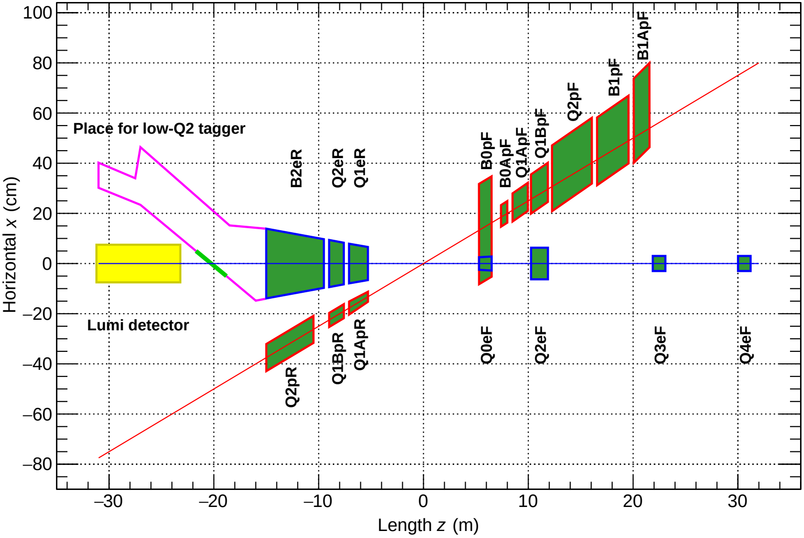

Geant4 model of luminosity monitor

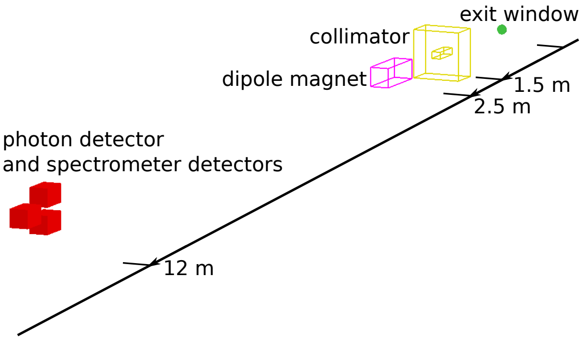

- Full Geant4 model of all essential part of luminosity monitor following the ZEUS design
- Photon exit window is located about 20 meters from interaction point
- Provides simulation chain from physics event generator to number of detected photoelectrons

Low-Q^2 tagger in Geant4

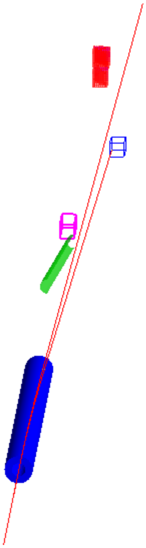

- The tagger is represented as the box right to the luminosity system
- Beam electron and scattered electron are passing through the B2eR dipole magnet
- The scattered electron is stopped in the tagger
- The edge of the tagger is placed 10 cm away from the axis of the beam, z = 27 m
- For the acceptance studies shown here, the tagger is implemented as a box 20x20 cm, length 35 cm
- The tagger stops the track and marks the hit (no secondaries)

Integration to the IR: photon exit window

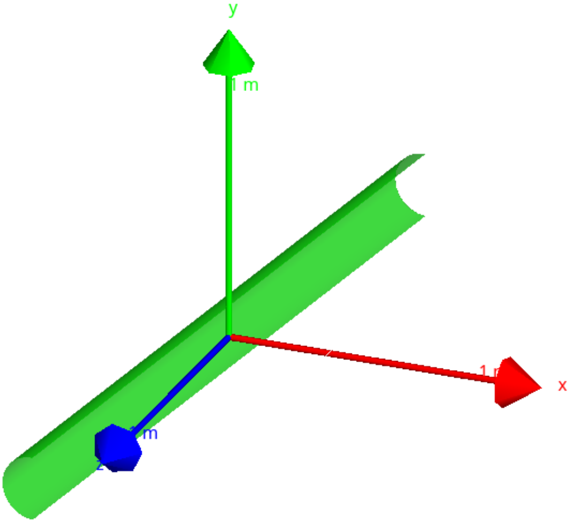

- Layer of passive material to convert bremsstrahlung photons to e^+e^- pairs
- Located 20 m downstream electron beam axis (exact location will depend on beam pipe geometry)
- Implemented as a half-cylinder of 1 mm thick aluminum, 10 cm radius and 100 mrad tilt along vertical y axis
- The tilt angle is motivated by synchrotron radiation studies
- Precise knowledge of the amount of material through which the photons travel is crucial
- More complex geometries suggested in discussions, like a dedicated pipe extruding from the beam pipe, ending with a more simple shape of the exit window

Luminosity pair spectrometer and direct photon detectors

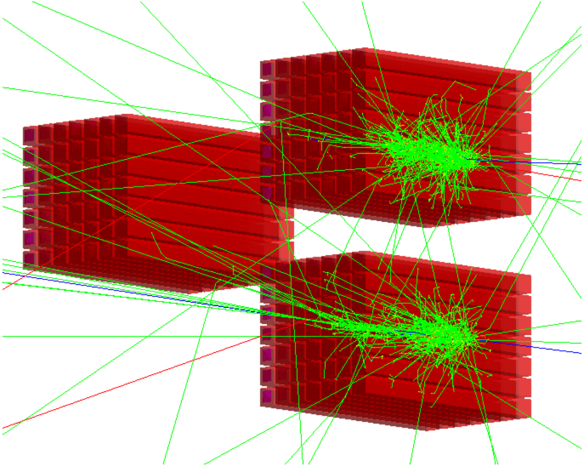

- Pair of calorimeters to detect converted e^+ and e^-
- Photon detector for non-converted photons is located behind
- Placed 11.35 m from the exit window
- Aperture between the detectors is 8.4 cm
- Shown is event with e^+ and e^- at 3 GeV, deflected by the magnet
- The need is for a fast calorimeter, segmented in x and y separately, with position resolution to identify pile-up events

Spectrometer acceptance as a function of photon energy

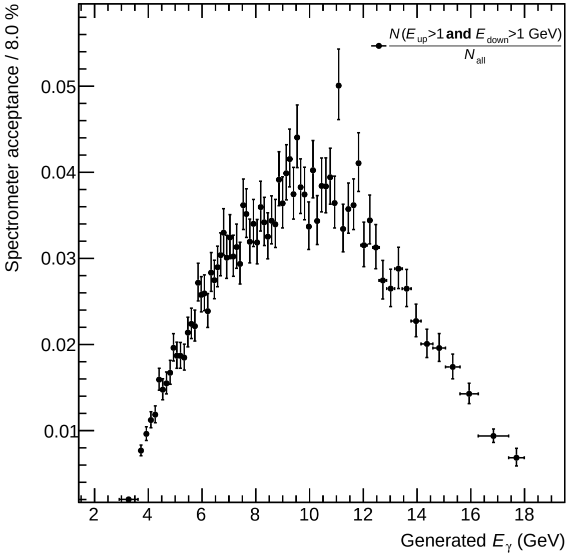

- The acceptance is ratio of number of events with coincident signal in both spectrometers to all generated events
- Shape is given by magnetic field of the dipole magnet
- Similar dependence of the acceptance was observed at ZEUS (with different field for different energies)
- Onset of the acceptance at higher energies eliminates background from synchrotron radiation
- Good energy resolution is necessary for the knowledge of the acceptance, as the event count, together with the acceptance and Bethe-Heitler cross section, give the luminosity

Kinematics of scattered electrons and relation to Q^2

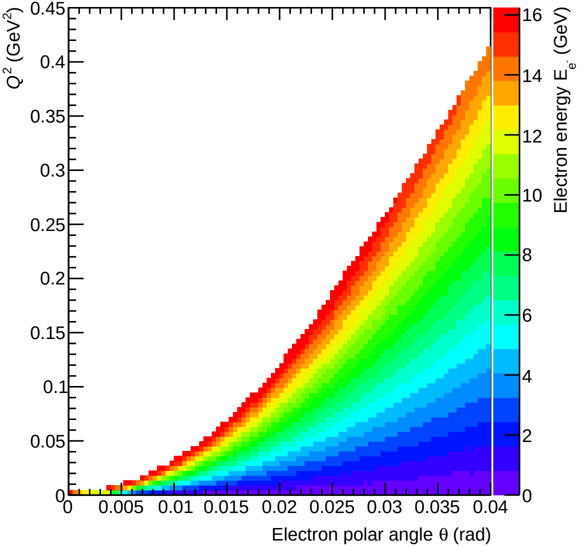

- Model of quasi-real photoproduction, the most general cross section for DIS scattered electrons, adopted from HERA studies
- Relation between electron scattering angle θ and Q^2
- The colors give the electron energy E_{e^-}
- Beam energy is 18x275 GeV
- Compatible with Fig. 2.20 in pCDR, page 90
- Values of low Q^2 are reached at very small angles
- The tagger will reconstruct the Q^2 from scattered electron energy and position on the tagger

Distribution of Q^2 for quasi-real photoproduction and Pythia6

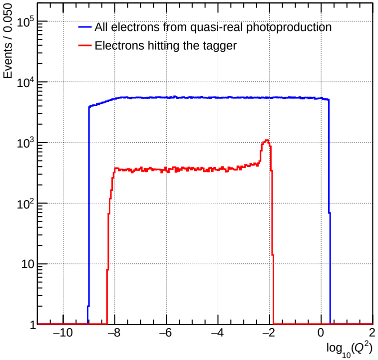

Figure: Quasi-real photoproduction

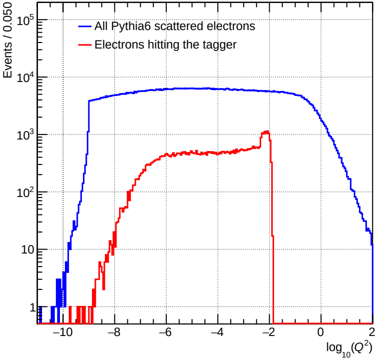

Figure: Q^2 of Pythia6 events

- Geant4 simulation of 1M events in each case
- Scattered electrons pass through the B2eR magnet
- The tagger counts the electrons which hit its volume
- The sample of electrons hitting the tagger also has a requirement for scattering angle θ to pass the B2eR aperture

- Quasi-real photproduction has range in x as $[10^{-12}, 1]$, range in y is $[1.6 \times 10^{-4}, 1]$ and range in Q^2 is $[10^{-9}, 2]$
- Approximately same intervals in x and y hold for Pythia6 sample, lower limit in Q^2 is also $\sim 10^{-9}$

Acceptance in Q^2

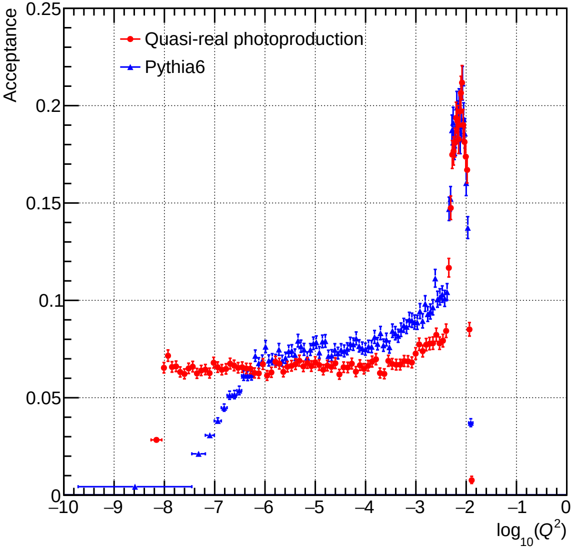

- Determined as a ratio of events hitting the tagger to all generated events
- Both models provide consistent results
- The acceptance has onset at $Q^2 \sim 10^{-2}$ GeV^2 (with decreasing Q^2)
- Lower limit of the acceptance is $Q^2 \lesssim 10^{-7}$ GeV^2

Effect of beam angular divergence and emittance to the Q^2

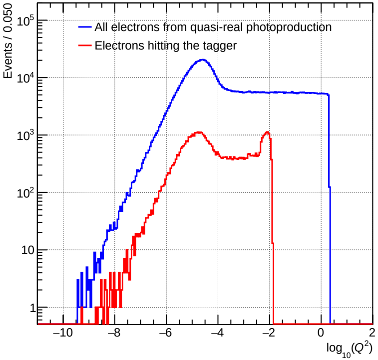

Figure: Quasi-real photoproduction

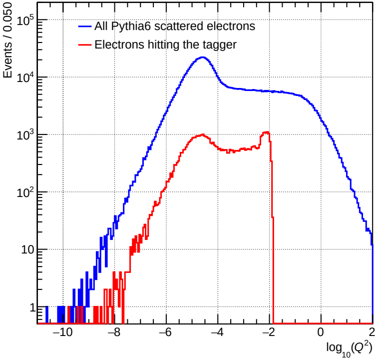

Figure: Q^2 of Pythia6 events

- The same simulations as on previous pages
- But with beam effects included with pCDR RMS values
- Vertex position is generated with RMS in x, y and z (Gaussian distribution)
- IP RMS beam size σ_x = 236 µm, σ_y = 16.2 µm, $\Delta\theta$ = 200 µrad
- RMS bunch length σ_z = 1.7 cm

- Angular divergence in applied as Gaussian smearing in angles ($\Delta\theta$), separately in x and y
- Horizontal and vertical beam divergence: RMS $\Delta\theta_x$ = 163 μrad, RMS $\Delta\theta_y$ = 202 μrad
- Similar shape was observed at HERA

Effect of beam divergence and emittance to the acceptance in Q^2

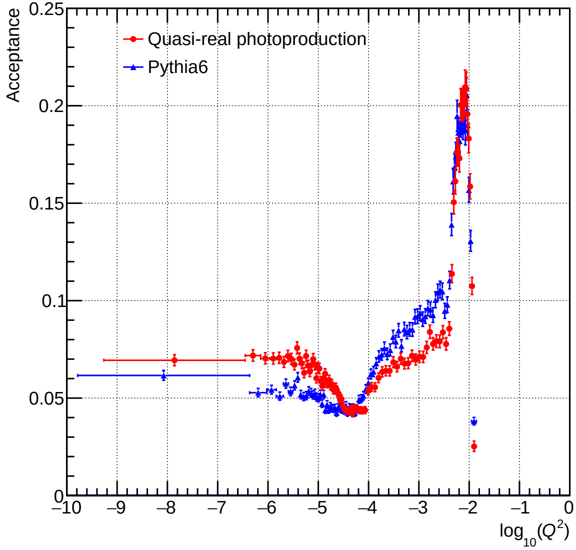

- Same analysis as for the version without beam effects
- No change in upper limit of the acceptance
- More complicated shape, a dip between 10^{-5} and 10^{-4}
- Much less events at very low Q^2, resulting in long bins
- Could indicate a systematic shift towards larger Q^2 in presence of beam effects

Hit position on the front face of the tagger

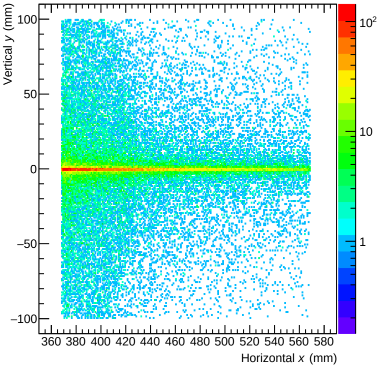

Figure: No beam effects

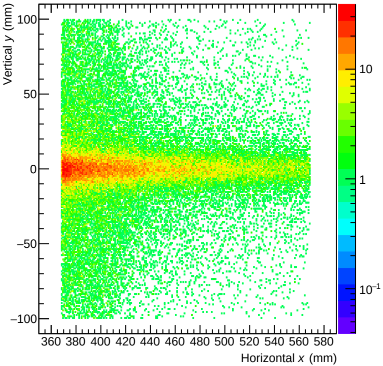

Figure: Beam effects included

- Coordinate position of electrons hitting the tagger on the front face of the tagger
- Most of the electrons are confined in horizontal plane
- Most hits take place in positions closer to the beam
- Beam effects cause smearing in observed positions

- The tagger has to reconstruct the Q^2 from electron hit position and its energy
- Tracking layers in front of the calorimeter will be necessary for position reconstruction
- Precision in Q^2 will have a large contribution from beam effects

Summary

- A fast sampling calorimeter is required both for luminosity monitor and low Q^2 tagger
- The tagger also needs a dedicated tracking layers in front of it
- Simulations are done with preliminary versions of the calorimeters
- Large event rates are expected for luminosity monitor, $\sim$100 MHz
- A set of event generators provide input events to the simulations both for luminosity monitor and the tagger
- Effects of beam emittance and angular divergence are implemented, including the Pythia6 sample
- Work in progress to implement effects of proton beam and crab cavities
- Ready to synchronize with fully realistic models of the detectors
- Codes for Geant4 simulations are here: https://github.com/adamjaro/lmon
- Codes for event generators are here: https://github.com/adamjaro/eic-lgen

Backup

Generator *lgen* based on Bethe-Heitler formula

- Bremsstrahlung photons and scattered electrons are generated using cross section as a function of photon energy E_γ and polar angle θ_γ
- Parametrization used at ZEUS is given in terms of electron and proton beam energy E_e and E_p

$$\frac{d\sigma}{dE_\gamma} = 4\alpha r_e^2 \frac{E'_e}{E_\gamma E_e}\left(\frac{E_e}{E'_e} + \frac{E'_e}{E_e} - \frac{2}{3}\right)\left(\ln\frac{4E_p E_e E'_e}{m_p m_e E_\gamma} - \frac{1}{2}\right) \tag{1}$$

- Scattered electron energy is constrained as $E'_e = E_e - E_\gamma$
- Equivalent parametrization from H1 is in terms of $y = E_\gamma/E_e$ and center-of-mass energy s

$$\frac{d\sigma}{dy} = \frac{4\alpha r_e^2}{y}\left[1 + (1-y)^2 - \frac{2}{3}(1-y)\right]\left[\ln\frac{s(1-y)}{m_p m_e y} - \frac{1}{2}\right] \tag{2}$$

- Angular distribution of the photons is given in terms of angle θ_γ relative to electron beam

$$\frac{d\sigma}{d\theta_\gamma} \sim \frac{\theta_\gamma}{\left((m_e/E_e)^2 + \theta_\gamma^2\right)^2} \tag{3}$$

ZEUS: Eur.Phys.J. C71 (2011) 1574, H1: H1-04/93-287

Model of photon detector

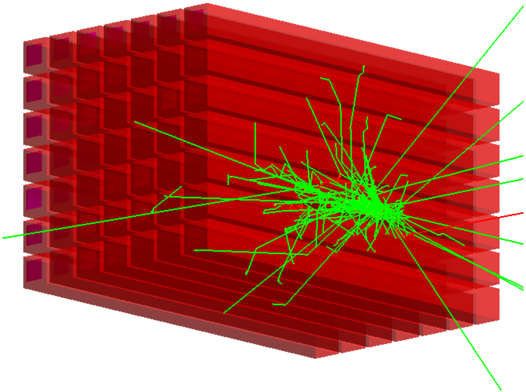

- Detects direct photons not converted on the exit window
- Placed along beam line (zero degree) 11.85 m behind the exit window
- Calorimeter is composed of 7×7 $PbWO_4$ cells
- Each cell consists of 3×3 cm casing made of carbon fiber, 2 mm thick, holding the $PbWO_4$ crystal inside
- Length of each cell is 35 cm, same for casing and crystal
- Only the crystals, shown in red, are sensitive volume
- Response to a 1 GeV photon is shown on the plot

Pair spectrometer detectors

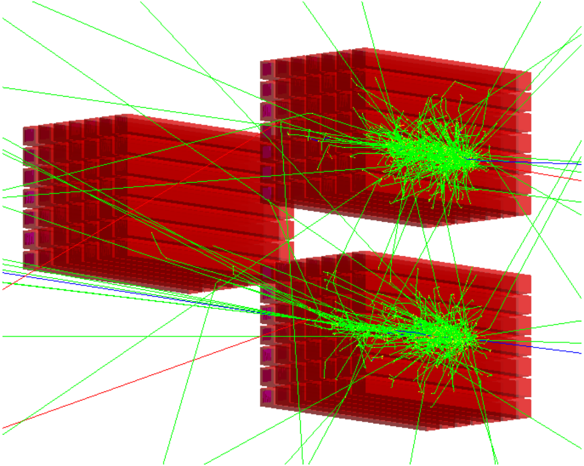

- Pair of calorimeters to detect converted e^+ and e^-
- Same construction as the photon detector
- Placed 11.35 m from the exit window
- Aperture between the detectors is 8.4 cm
- Photon detector is located behind
- Shown is event with e^+ and e^- at 3 GeV, deflected by spectrometer magnet

Predictions for event rates based on Bethe-Heitler cross section, pCDR luminosity and simulated efficiency

- Expected event rate f is given by Bethe-Heitler bremsstrahlung cross section σ_{BH}, luminosity L, and efficiency to observe a given process ϵ

$$f = \sigma_{\mathrm{BH}} \times L \times \epsilon \tag{4}$$

- The cross section σ_{BH} is determined from ZEUS parametrization used to generate events for simulation
- Simulated 10^5 events for E_e = 18 GeV and E_p = 275 GeV and minimal bremsstrahlung photon energy of 1 GeV
- The corresponding σ_{BH}= 129.6 mb
- Luminosity quoted in pCDR for this energy is L = 1.45×10^{33} cm^{-2}s^{-1} = 1.45×10^{6} mb^{-1}s^{-1}
- This is the highest value assumed in pCDR with strong hadron cooling and high divergence configuration
- Event rates f will be given for signal in direct photon detector, signals in spectrometer detectors and coincidence in the pair spectrometer

Results on event rates

- Individual efficiencies ϵ are obtained as a ratio of selected events having energy deposition over the threshold, to all simulated events
- Each event rate f is obtained by putting the particular ϵ into Eq. 4, $f = \sigma_{\mathrm{BH}} \times L \times \epsilon$
- Signal in direct photon detector, deposited energy over 1 GeV
  - $\epsilon_{\mathrm{phot}} = 0.8998 \pm 0.0009$
  - $f_{\mathrm{phot}} = 169.08$ MHz
- Signal in upper spectrometer detector, deposited energy over 1 GeV
  - $\epsilon_{\mathrm{up}} = 0.0293 \pm 0.0005$
  - $f_{\mathrm{up}} = 5.51$ MHz
- Signal in down spectrometer detector, deposited energy over 1 GeV
  - $\epsilon_{\mathrm{down}} = 0.0292 \pm 0.0005$
  - $f_{\mathrm{down}} = 5.48$ MHz
- Coincident signal in both spectrometer detectors, up and down detectors have at least 1 GeV of deposited energy
  - $\epsilon_{\mathrm{pair}} = 0.0116 \pm 0.0003$
  - $f_{\mathrm{pair}} = 2.19$ MHz
- We can expect large rates, luminosity monitor will have no problems with event statistics

Optical properties and light detection in model of $PbWO_4$ crystal

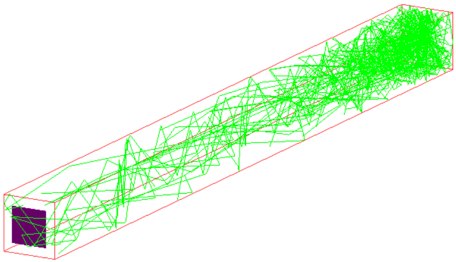

Figure: One calorimeter cell with 2 MeV deposition on the far side (facing the IP) and optical photon detector (magenta) on the opposite side. Optical photons are shown as green lines.

- Scintillation light yield is 200 per MeV with 6 ns decay constant (Knoll textbook)
- Wavelenght 420 nm (peak of emission as measured for ALICE)
- Optical properties approximately according to ALICE TDR
  - Uniform across 350 - 800 nm
  - Refractive index 2.4, absorption length 200 cm
  - Reflectivity 0.8, efficiency 0.9
- Detection by PIN diode, magenta square in the drawing
  - Silicon of 17×17 mm^2 area, 300 μm thickess (following ALICE device)
  - Reflectivity of optical boundary from the crystal is 0.1
  - Quantum efficiency is 0.8
  - Detected photon creates one photoelectron of signal (after applying quantum efficiency)
  - Number of photoelectrons is the output of the detector

Reconstructing the energy from number of photoelectrons

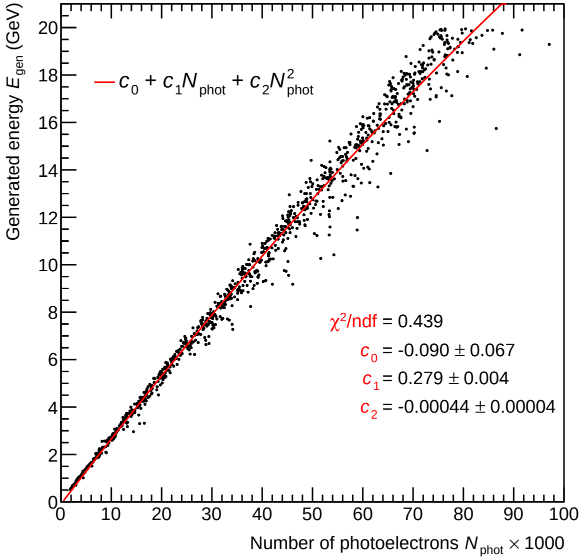

- Plot shows energy of generated photon entering the detector and number of photoelectrons from all cells
- One point is one event (1000 in total)
- Generated photons have uniform energy distribution in 0.5 - 20 GeV
- Fit is made by quadratic polynomial, not ideal but works
- Coefficients c0, c1, c2, known from the fit, allow to calculate reconstructed energy from number of photoelectrons

Reconstructed and generated energy

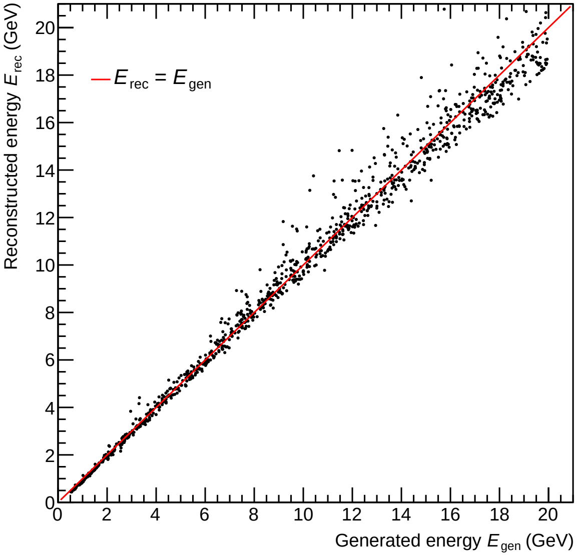

- Reconstructed energy is calculated from number of photoelectrons using c0, c1 and c2 determined from the fit on previous page
- Reconstructed energy is then compared to generated energy, same simulation of 1000 events
- Spread gets larger at energies beyond 10 GeV
- Caused by fluctuations in number of photoelectrons

Relative energy resolution

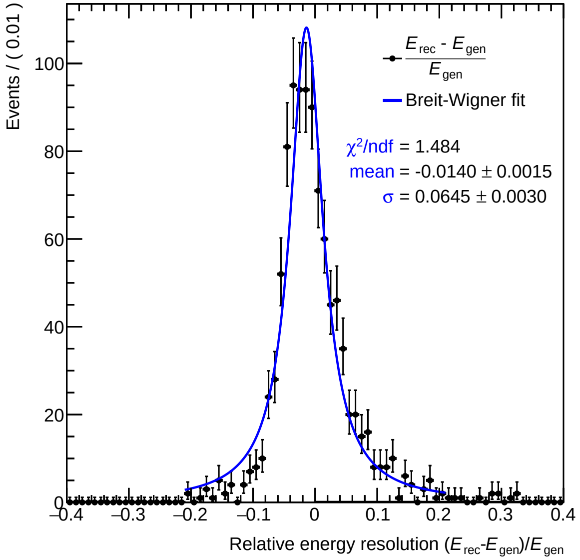

- Relative energy resolution is obtained as distribution of difference between reconstructed and generated energy, divided by generated energy
- Fit is made by Breit-Wigner distribution
- Width σ gives the relative resolution of 6.5% for energy in 0.5 - 20 GeV
- ALICE is quoting 3% over 0.2 - 10 GeV
- Difference is likely due to different energy range and conservative approach to light collection
- Light collection will need particular care because of limited light yield

Model of quasi-real photoproduction

- Event generator implemented to *lgen* using one photon exchange cross section from HERA study in Conf.Proc. C790402 (1979) 1-474
- The parametrization for quasi-real photoproduction in low-Q^2 approximation (Eq. II.6 in HERA study) is

$$\frac{\mathrm{d}^2\sigma}{\mathrm{d}x\mathrm{d}y} = \frac{\alpha}{2\pi} \frac{1+(1-y)^2}{y} \sigma_{\gamma p}(ys) \frac{1-x}{x} \;(\mathrm{mb}) \tag{5}$$

- The total photon-proton cross section $\sigma_{\gamma p}$ is used from Regge fit in Phys.Lett. B296 (1992) 227-232:

$$\sigma_{\gamma p}(ys) = 0.0677(ys)^{0.0808} + 0.129(ys)^{-0.4525} \;(\mathrm{mb}) \tag{6}$$

- Equation 5, with input from Eq. 6, is used to generate values of Bjorken x and inelasticity y
- Kinematics is then applied to generate the electrons with output to TX or Pythia6 format
- Similar procedure was used for H1 low-Q^2 tagger in H1-04/93-287 (1993)

Kinematics of electrons hitting the tagger

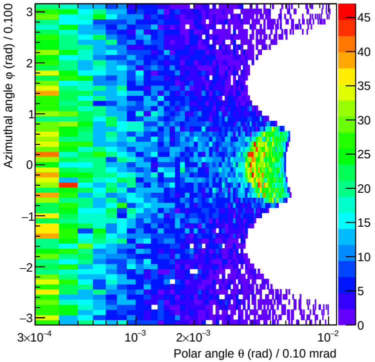

Figure: Electrons scattering angle θ and azimuthal angle φ for electrons hitting the tagger

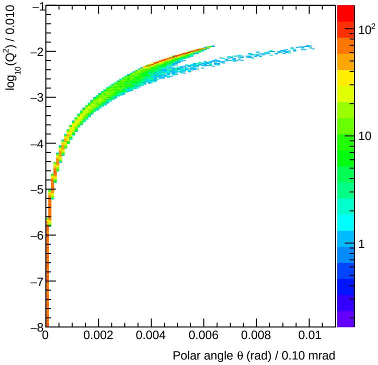

Figure: Q^2 and θ for electrons hitting the tagger

- Azimuthal angles φ are generated as uniform
- Electrons can reach the tagger from any ϕ
- Values of Q^2 and scattering angle θ for electrons which hit the tagger are strongly correlated